Published in final edited form as:
Environ Sci Technol. 2012 January 3; 46(1): 348–359. doi:10.1021/es201239f.

A Microarray Biosensor for Multiplexed Detection of Microbes Using Grating-Coupled Surface Plasmon Resonance Imaging

Gregory Marusov[1], **Andrew Sweatt**[1], **Kathryn Pietrosimone**[1], **David Benson**[1], **Steven J. Geary**[2,4], **Lawrence K. Silbart**[3,4], **Sreerupa Challa**[3,4], **Jacqueline Lagoy**[1], **David A. Lawrence**[5], and **Michael A. Lynes**[1,4,*]

Michael A. Lynes: michael.lynes@uconn.edu

[1]Department of Molecular and Cell Biology, The University of Connecticut, 91 North Eagleville Road, Storrs, CT 06269-3125

[2]Department of Pathobiology, The University of Connecticut, 91 North Eagleville Road, Storrs, CT 06269-3125

[3]Department of Allied Health Sciences, The University of Connecticut, 91 North Eagleville Road, Storrs, CT 06269-3125

[4]The Center of Excellence For Vaccine Research, The University of Connecticut, 91 North Eagleville Road, Storrs, CT 06269-3125

[5]Wadsworth Center, NY Department of Health, Albany, NY 12208

Abstract

Grating-coupled surface plasmon resonance imaging (GCSPRI) utilizes an optical diffraction grating embossed on a gold-coated sensor chip to couple collimated incident light into surface plasmons. The angle at which this coupling occurs is sensitive to the capture of analyte at the chip surface. This approach permits the use of disposable biosensor chips that can be mass-produced at low cost and spotted in microarray format to greatly increase multiplexing capabilities. The current GCSPRI instrument has the capacity to simultaneously measure binding at over 1000 unique, discrete regions of interest (ROIs) by utilizing a compact microarray of antibodies or other specific capture molecules immobilized on the sensor chip. In this report, we describe the use of GCSPRI to directly detect multiple analytes over a large dynamic range, including soluble protein toxins, bacterial cells, spores, and viruses, in near real-time. GCSPRI was used to detect a variety of agents that would be useful for diagnostic and environmental sensing purposes, including macromolecular antigens, a non-toxic form of *Pseudomonas aeruginosa* exotoxin A (ntPE), *Bacillus globigii*, *Mycoplasma hyopneumoniae*, *Listeria monocytogenes*, *Escherichia coli*, and M13 bacteriophage. These studies indicate that GCSPRI can be used to simultaneously assess the presence of toxins and pathogens, as well as quantify specific antibodies to environmental agents, in a rapid, label-free and highly multiplexed assay requiring nanoliter amounts of capture reagents.

Keywords

multi-analyte detection; pathogen detection; cell and protein microarray; high-throughput SPR biosensor; grating-coupled surface plasmon resonance imaging; multiplexed immunoassay

*Address correspondence to: Michael A. Lynes, Ph.D., U-3125, University of Connecticut,Department of Molecular and Cell Biology, 91 North Eagleville Road, Storrs, CT 06269-3125. Phone: (860)486-4350 Fax: (860)486-4331.

Supporting Information Available: Additional figures and experimental details regarding GCSPRI assay optimization can be found in supporting information. This information is available free of charge via the Internet at http://pubs.acs.org/.

Introduction

On-site monitoring of environmental samples poses a tremendous challenge due to the vast number of potential microbes (bacteria, viruses, and fungi), and the heterogeneous nature of each microbe in terms of toxin synthesis, antigenicity, and physical characteristics. Traditionally, detecting and identifying bacterial pathogens relies upon culture of the organism, colony morphology evaluation, and identification of characteristic nucleic acid sequences, biochemical markers, and antigenic signatures associated with the microbe [1], but these assays are complex, labor intensive and time-consuming. Typical sandwich-style immunoassays are impractical for continuous monitoring, since they require significant incubation and sample processing times, are of limited throughput, and require costly fluorescent conjugates or enzyme-labeled reagents. Moreover, reporter labels required for many immunoassay detection systems may alter antibody affinity, specificity or stability. Polymerase Chain Reaction (PCR)-based techniques enable sensitive and specific identification of an organism by rapid amplification of specific DNA/RNA sequences, but quantitative real-time PCR data interpretation is complex, making automation difficult, and the number of analytes that can be detected simultaneously is limited [2]. Recently, high-density oligonucleotide microarray technologies and high-throughput “next-generation” sequencing have been utilized to increase multiplexing capabilities of nucleic acid-based pathogen detection, but these approaches require expensive instrumentation and consumables as well as extensive user training and data analysis [3-7]. Surface plasmon resonance (SPR) technology has emerged as a promising method of molecular detection and analysis that is being developed for a wide variety of applications. SPR analysis takes advantage of the high specificity and affinity of antibodies to directly detect unlabeled analytes in near real-time without requiring sample purification or enrichment, competitive immunoassay set-ups, or the use of labeled reagents. SPR measurements are based on energy transfer from a *p*-polarized illuminating light source to a metal surface at ametal/dielectric interface [8]. This energy transfer is dependent upon matching properties of the incident light (wavelength, incidence angle, and phase velocity) to the resonance requirements of the metal electrons. When these resonance conditions are met, propagating evanescent electromagnetic waves known as surface plasmons are produced, and as a consequence the intensity of the light reflected from the metal surface is decreased [9]. SPR instrument platform configurations are generally differentiated by their use of wavelength-, angular-, intensity-, polarization-, or phase-modulation as the basis of measurement [10]. If the illuminating light in an SPR system is held at a constant wavelength, a minimum in the reflected light intensity (and maximum SPR coupling) will occur at a specific angle of incidence (the SPR angle). Analyte binding to the sensor surface induces a change in refractive index at that surface and influences this resonant angle, causing a shift in the SPR angle. Conventional SPR analysis based on the Kretschmann design [11] has been used in a number of different instrument platforms that utilize the high refractive index of a prism to reduce the phase velocity of the incident light and achieve the required resonance conditions.

A number of different SPR biosensors, usually based on a prism-coupled configuration, have been described for the detection of various chemical and biological analytes [12]. Prism-coupled SPR has been used to detect a variety of human and agricultural pathogens in a label-free manner, including *Staphylococcus aureus* [13], *Escherichia coli* O157:H7 [14], *Salmonella enterica* [15], *Vibrio cholerae* [16], *Cryptosporidium parvum* [17], *Listeria monocytogenes* [18], *Phytophthora infestans* sporangia [19], tobacco mosaic virus [20], and hepatitis A virus [21]. These systems can also detect pathogen-associated molecules such as Staphylococcal enterotoxins SEB [22] and SEA [23] and human antibodies against Epstein-Barr virus [24] and hepatitis B virus [25]. However, drawbacks of the prism-coupled configuration include the limited number of simultaneous measurements that can be

performed, the challenge of manufacturing a sensor chip with an ultrathin gold film to high tolerances, and the requirement to optically couple the prism to the sensor chip surface. Prism-coupled SPR instruments with multiple sensor elements or sample channels for detection of multiple analytes or parallel analysis of multiple samples have been described in the literature. For example, a 24-analyte instrument was developed that employs three channels for each prism-based sensor element, and combines eight of these sensor elements [26]. The number of sensing channels has also been increased by applying wavelength division multiplexing (WDM), which relies upon excitation of surface plasmons at different wavelengths in different sensing channels [27, 28]. An eight-channel SPR biosensor based on Kretschmann geometry, spectral interrogation, and WDM was shown to be capable of simultaneous detection of four bacterial pathogens [29].

Another approach for developing high-throughput SPR sensors involves SPR imaging (SPRi), also called “SPR microscopy”, which utilizes spatially resolved measurements of sensing spots to analyze refractive index changes at discrete regions of the sensor chip surface [30]. A microfluidic chip was integrated with a two-dimensional SPR phase imaging system for developing a three by three microarray immunoassay [31]. SPRi systems utilizing polarization contrast and spatially patterned SPR multilayers have been shown to support a total of 108 sensing channels [32]. Most existing SPRi instruments are based on prism coupling and intensity modulation, and measure intensity variation of reflected light at a fixed angle of incidence [30]. A commercial SPRi instrument (*i*SPR, IBIS Technologies B.V., Hengelo, The Netherlands) based on prism coupling and operating in continuous angle-scanning mode was recently demonstrated to have a 10 times larger dynamic range compared to a fixed angle SPRi instrument (SPRimager®II, GWC Technologies, Madison, WI)[33].

In contrast to prism-coupled SPR, grating-coupled surface plasmon resonance imaging (GCSPRI) utilizes an optical diffraction grating embossed on a gold-coated sensor chip to couple collimated incident light into surface plasmons and generate a measurable SPR angle [34, 35]. While the standard Kretschmann configuration employs optical illumination from the opposite side of the sensor chip binding surface, GCSPRI measures the optical changes from the same side of the sensor surface as the molecular binding events. For this reason, GCSPRI lends itself to direct imaging of the surface and enables highly parallel measurements from the same micro volume sample. The molded plastic optical gratings of GCSPRI sensor chips can be mass-produced at very low cost using existing compact disk (CD) manufacturing technologies [34, 36]. This represents an advantage over prism-based SPR applications that require manufacture of specialized prisms, thin plasmon-active metal films of a very precise thickness, and optically suitable substrates in order to achieve the necessary conditions of attenuated total internal reflection [36, 37]. Robotic microspotting technology can produce microarrays of capture molecules, that only consumenanoliter quantities of each reagent per chip, and multiple sensor chips can be printed in parallel, improving assay-to-assay reproducibility. The instrument used in the studies reported here has the capacity to simultaneously measure binding events at 1024 unique and spatially discrete regions of interest (ROIs) on a 1 cm2 diffraction grating by utilizing a compact microarray of antibodies or other specific capture molecules immobilized on the sensor chip. Such high content assays are invaluable for screening when the composition of the sample is likely to be complex (e.g. environmental samples). The results reported here demonstrate that GCSPRI can be used to simultaneously assess the presence of toxins and microbes in biological samples in a rapid, label free, and highly multiplexed assay.

Materials and Methods

GCSPRI Instrumentation

The optical configuration of the angular modulation GCSPRI instrument used has been previously described [35]. Briefly, GCSPRI uses a scanning optical head moved by an angle encoder to illuminate the sensor chip at a series of sequential angles from 17.5° to 21° (relative to vertical) in 0.05 degree steps. Images of the reflected light at each of the illuminating angles are captured with a CCD camera. The light source is a single 867-nm light emitting diode (LED) [34]. The initial scan captures images at 91 angles and then uses a computational algorithm to calculate the SPR curve and the minimum in reflected light intensity, known as the SPR angle. Biomolecular interactions are monitored in real-time using continuous angle-scanning to measure the shift in the SPR angle resulting from analyte binding to the sensor chip. Data shown represents the shift in the GCSPRI angle in millidegrees (mDeg) as a consequence of analyte binding to the sensor surface.

Reagents

Antibodies were purchased from a variety of sources: affinity-purified polyclonal rabbit IgG anti-*Bacillus globigii* and anti-*Erwinia herbicola* (Tetracore, Inc, Rockville, MD), mouse IgG2a anti-M13 (GE Healthcare Life Sciences, Piscataway, NJ), mouse IgG2a (clone LZF7), mouse IgG1 (clone LZH1), and affinity-purified polyclonal rabbit IgG anti-*Listeria monocytogenes* (AbD Serotec, Raleigh, NC), affinity-purified polyclonal rabbit IgG anti-lipotechoic acid (AbD Serotec), affinity-purified polyclonal goat IgG anti-*Escherichia coli* (Abcam Inc, Cambridge, MA), mouse serum anti-ovalbumin and goat serum anti-mouse IgG (Southern Biotechnology Associates, Inc, Birmingham, AL), mouse IgG (for 32x32 array) (Biomeda Corporation, Foster City, CA), mouse IgG anti-human Hsp70 (Enzo Life Sciences, Plymouth Meeting, PA), and mouse IgG2a anti-human IL-2 and mouse IgG1 anti-human CD3e (R & D Systems, Minneapolis, MN).

Chicken ovalbumin (Ova), bovine serum albumin (BSA), Tween 20, cold-water teleostean gelatin, porcine and murine IgG (for *M. hyopneumnia* experiments) were purchased from Sigma-Aldrich, Inc (St. Louis, MO). Superblock was obtained from Pierce Biotechnology (Rockford, IL) and Stabilcoat was purchased from Surmodics, Inc (Eden Prairie, MN). Non-toxic *Pseudomonas aeruginosa* exotoxin A (ntPE) and the porcine anti-ntPE IgG cognate antibody were produced as previously described [38]. Anti-*M. hyopneumoniae* serum was collected from a pig experimentally infected with the virulent *M. hyopneumoniae* strain 232. Pre-immune IgG, anti-*M. hyopneumoniae* IgG, and anti-ntPE IgG were purified from porcine sera using Protein A columns (Pierce) according to standard protocols provided by the manufacturer. *M. hyopneumoniae* was grown and harvested as previously described [39], and a microbe lysate was prepared by 10 successive dry ice/methanol freeze-thaw cycles, followed by filtration through a 0.22 μm filter (Fisher Scientific, Pittsburgh, PA). Protein concentration was determined by the BCA assay (Pierce). *Bacillus globigii* (ATCC #49760, American Type Culture Collection, Mannassas, VA) was cultured to log phase in Tryptic Soy Broth (TSB) or on TSB agar (Becton Dickinson, Franklin Lakes, NJ) according to conditions described in the ATCC Bacterial Culture Database (ATCC 2004). Where indicated, *Bacillus* cells were fixed in 0.5% paraformaldehyde for 1 hour in order to create a bacterial stock suspension of known concentration for use in replicate experiments. *E. coli* MC1061 was provided by Dr. Debby Laukens (Ghent University, Belgium) and was cultured in yeast tryptone medium (YTA). *L. monocytogenes* was originally isolated from a meningitis patient and has been maintained as previously described [40]. *Listeria* was cultured to mid-log phase in Brain Heart Infusion (BHI) broth, resuspended in PBST, and heat-killed as previously described [15]. M13K07 helper phage was purchased from New England Biolabs (Beverly, MA).

GCSPRI sensor chip preparation

GCSPRI sensor chips (Ciencia, Inc. East Hartford, CT) have a 1 cm active sensing area that consists of a plastic optical grating (period of 867 nm and groove depth of 40 nm) coated with a thin (~ 80 nm) layer of gold. Sensor chips were cleaned using 70% ethanol in deionized, distilled water and then air-dried. Replicate spots of capture molecules were deposited on the unmodified gold surface of GCSPRI sensor chips either manually or using a robotic spotter. Manual spotting was done using a Schleicher & Schuell (Keene, NH) MicroCASTer™ pin-spotter, which deposits 20-70 nL. An OmniGrid Micro robotic spotter (Genomic Solutions, Ann Arbor, MI) using an ArrayIt Stealth Micro Spotting Pin (TeleChem International, Inc., Sunnyvale, CA), size SMP7B (delivers 3 nL per spot) or SMP3B (delivers 0.9 nL per spot), was used to print larger microarrays of spots approximately 255 mm or 110 mm in diameter, respectively. Spotted sensor chips were incubated in a humid chamber for at least 30 minutes and air dried or stored in a vacuum desiccator at 4° C until use.

GCSPRI Assays

For GCSPRI experiments, the regions of interest (ROIs) were defined in the software to correspond to immobilized spotted capture reagents on each sensor chip microarray. Templates of the ROIs were drawn such that each target ROI covered at least 85% of the visible capture reagent. Local reference ROIs were drawn on unspotted gold adjacent to each target ROI. A general GCSPRI detection protocol consisted of a blocking step, a buffer wash with PBS or PBS containing 0.5% Tween-20 (PBST) to establish a pre-sample GCSPRI baseline, sample delivery, and a final buffer wash to establish the post-sample GCSPRI baseline. Delivering the blocking solution (2% BSA, 10% Superblock, or 5% cold water teleostean gelatin) at an initial rapid flow rate of at least 1 mL/min prevented readsorption of non-immobilized capture molecules to other regions of the chip, and flow was subsequently paused for at least 15 minutes to allow the blocking solution to interact with the sensor chip surface and to block any remaining sites where non-specific adsorption could occur. Buffer composition was maintained throughout each experiment and all assays were performed at room temperature. Data analysis was performed as previously described [35, 41].

Statistical analysis

End-point GCSPRI angle shifts at replicate ROIs are indicated as mean ± standard deviation, and statistical significance ($p < 0.05$) was determined by Student's *t*-test using Graphpad Prism 4.0 for Macintosh (GraphPad Software, Inc., La Jolla, CA).

Results

Microarray Printing

In most experiments, capture molecules were immobilized by passive adsorption in microarray format using an OmniGrid Micro robotic spotter (Genomic Solutions**,** Ann Arbor, MI). After microarray printing, a sample flowcell (~40 μL volume) is created by adhering a gasketed window to the chip surface (Figure 1a). Most arrays were printed using a size SMP7B Stealth Micro Spotting Pin (Arrayit Corporation, Sunnyvale, CA), but by using a smaller-tipped microspotting pin (size SMP3B), more than 1000 different capture spots could be immobilized on a 32x32 array within the 1 cm^2 active area of a sensor chip (Figure 1b, blue circles). The packing density of these capture regions of interest (ROIs) is determined by the 10 μm distance surface plasmons propagate in gold [42], the requirement for interspersed local reference ROIs (Figure 1b, red circles) to correct for bulk changes in refractive index and non-specific binding, the resolution of the imaging optics, and the

potential for cross contamination of capture reagents between adjacent ROIs. The 32x32 array shown was composed of mouse IgG ROIs and BSA ROIs arranged in a specific pattern with high value ROIs immediately adjacent to negative controls. Large angle shifts resulting from goat anti-mouse IgG antibody binding to mouse IgG ROIs do not affect the SPR signal at adjacent negative control BSA ROIs or interspersed bare gold reference ROIs (Figure 1c), indicating that each ROI functions as an independent measure of analyte presence in the sample.

Detection of Soluble Analytes; Toxins and Antibodies

Immobilization of affinity-purified anti-ntPE porcine IgG on a GCSPRI sensor chip allowed for direct detection of ntPE (10 μg/mL) (Figure S1). On the same chip, there was virtually no binding of ntPE to porcine IgG purified in the same manner from a non-immunized animal. By reversing the configuration of the assay and immobilizing ntPE on the biosensor chip, it was also possible to detect cognate antibody from serum samples. Flowing porcine IgG from naïve animals over immobilized ntPE resulted in negligible GCSPRI angle shifts at both BSA (control) and ntPE ROIs, but subsequent flow of equally diluted IgG from an ntPE-immunized pig caused angle shifts for ntPE ROIs only (Figure 2a). This binding is quantitative in nature, as increasing concentrations of immobilized ntPE captured increasing levels of anti-ntPE IgG from the sample. In the same experiment, subsequent flow of an anti-porcine IgG secondary antibody doubled the angle shift at ntPE ROIs, further amplifying the assay sensitivity.

We also used GCSPRI to detect the presence of pathogen-specific antibodies against virulent *M. hyopneumoniae*. Total protein from *M. hyopneumoniae* freeze/thaw lysate was immobilized on a single sensor chip at a range of concentrations, and total IgG was isolated from *M. hyopneumoniae*-infected porcine sera and flowed over the chip as analyte. At the highest concentration of immobilized antigenic protein (1 mg/mL in 1% Stabilcoat), subsequent flow of an anti-porcine secondary antibody over the captured the anti-*M. hyopneumoniae* IgG resulted in a maximal angle shift of approximately 72-82 mDeg (Figure 2b). The same anti-*M. hyopneumoniae* IgG preparation was immobilized on another sensor chip along with appropriate negative controls. *M. hyopneumonia*e lysate was flowed over the chip and produced significant binding at only the anti-*M. hyopneumoniae* IgG ROIs (62.7 mDeg) (Figure 2c). There was minimal non-specific binding of *M. hyopneumoniae* protein to naïve porcine IgG or murine IgG.

Detection of Particulate Analytes; Bacteria

Detection of pathogenic bacteria is critical for many applications in the food industry, in pharmaceutical manufacturing, for water and environmental quality control, and for clinical diagnosis and biosecurity purposes[43]. GCSPRI was used to detect representative pathogens: *Escherichia coli*, *Listeria monocytogenes,* and *Bacillus globigii* (as a surrogate for *B. anthracis*). Viable *E. coli* MC1061 ($1x10^8$ CFU/mL in PBST) resulted in significant binding to goat polyclonal anti-*E. coli* antibody but not to the negative control ROIs on the same chip (Figure 3a).

The multiplexing capabilities of GCSPRI can also be applied for parallel screening of different antibodies and estimation of their relative affinity for a specific target. Two different monoclonal anti-*Listeria* antibodies, clones LZF7 and LZH1, and a rabbit polyclonal anti-*Listeria* antibody, were immobilized along with several different negative control antibodies at equivalent concentrations on a sensor chip in order to evaluate their relative abilities to detect *Listeria* by GCSPRI. A sample of intact heat-killed *Listeria* ($1.65x10^9$ cells/mL in PBST) resulted in much larger angle shifts with LZF7 (115 mDeg shift at 500 μg/mL ROIs) than with LZH1 or polyclonal antibody (21 mDeg and 43 mDeg

shifts, respectively) (Figure 3b). Moreover, serial dilutions of LZF7 showed a linear dose response, evidenced by doubling angle shifts of 31, 59, and 115 mDeg at 125, 250, and 500 μg/mL ROIs, respectively. Interestingly, the three anti-*Listeria* antibodies demonstrated slightly different relative affinities for *Listeria*, which was dependent on whether heat-killed, viable, or detergent-lysed *Listeria* was used **(**data not shown**).** Similar sample preparation-dependent differences in prism-based SPR detection of *E. coli* have been previously described [44].

In order to further evaluate the quantitative limits of detection for intact bacteria capture and detection, a range of concentrations of anti-*Bacillus globigii* antibody and negative control antibodies were immobilized on a sensor chip. *B. globigii* (4×10^7 cells/mL) was flowed over the sensor chip and assessed with GCSPRI. Immediately after this analysis, the chip was gently dipped in deionized H_20 to remove salts, air dried, and stored in a desiccated container under vacuum conditions at 4 °C until it was used for scanning electron microscopy (SEM) imaging. The diffraction grating that is formed on the GCSPRI chip was easily observed at a magnification of 17,000× (Supporting Figure S3) and was used as an internal reference scale. SEM images taken at 750× were of sufficient resolution to allow for enumeration of individual bacterial cells. The number of bacteria counted within each ROI was plotted against the observed angle shift at that ROI (Figure 3c). Based on linear correlation analysis of this data, approximately 90 captured bacterial cells are required to produce an SPR signal that is 2 S.D. above background. This result is consistent with results from experiments where bacteria at known concentrations were directly adsorbed to unmodified gold before GCSPRI analysis (data not shown).

Detection of Particulate Analytes; Viral Particles

We have also explored the capacity of GCSPRI to detect viral particles. To estimate the limit of detection (LOD) for viral particle detection, mouse anti-M13 antibody was immobilized on a sensor chip and a series of M13 bacteriophage samples were passed over the chip at 10-fold increasing concentrations. The baseline was reset after each sample to allow specific measurement of the angle shift for that concentration. While there was no observable change in SPR signal from a sample of 10^4 PFU/mL, a positive angle shift (2.54 mDeg at 1 mg/mL capture spots) was observed for sample concentrations as low as 10^5 PFU/mL (Figure 4a). Greater angle shifts were observed at spots of higher capture antibody concentration, and successive increasing viral loads yielded successively larger angle shifts. M13 mixed with aquarium water from a functioning freshwater fish tank was used to evaluate whether GCSPRI is capable of measuring viral load in complex environmental samples. Figure S2 shows that the angle shift resulting from approximately 2×10^9 PFU/mL is equivalent for viral particles in PBS or in fish aquarium water.

To be practical for continuous on-line monitoring of environmental samples, a multiplexed biosensor must be capable of detecting multiple analytes presented to the detector both simultaneously and at successive time intervals. Additionally, it is critical that binding at one ROI on the sensor chip does not affect the observed signals at other ROIs. To further evaluate the multiplexing capabilities of GCSPRI, anti-ovalbumin, anti-M13, and anti-*B. globigii* antibodies were immobilized at different ROIs on three replicate sensor chips. M13 (10^6 PFU/mL in PBS) was flowed over one sensor chip, resulting in an average angle shift of 2.9 mDeg at the ROIs with anti-M13 antibody and minimal binding to the other two irrelevant antibodies (Figure 4b**,** left group). The M13 sample was followed by subsequent exposure to ovalbumin (20 μg/mL in PBS), resulting in an angle shift of 8.96 mDeg at the anti-ovalbumin ROIs and negligible binding at other irrelevant ROIs (Figure 4b, right group). The same concentrations of M13 and ovalbumin were combined in PBS and delivered to a replicate sensor chip. An average shift of 2.22 mDeg was observed at the anti-

M13 ROIs, and an average shift of 8.91 mDeg was seen at the anti-ovalbumin ROIs (Figure 4c, left group). When equivalent concentrations of the two analytes were diluted together in freshwater aquarium water and flowed over a third replicate sensor chip, average shifts of 2.11 mDeg at the anti-M13 ROIs and 8.0 mDeg at the anti-ovalbumin ROIs were observed (Figure 4c, right group).

Discussion

We describe a novel approach to pathogen detection that capitalizes upon several advantages associated with GCSPRI: (1) grating-coupled SPR permits the use of disposable sensor chips that can be mass-produced at low cost; (2) SPR imaging enables high-throughput analysis of over 1000 individual ROIs in a single assay, enabling the interrogation of a sample for hundreds of analytes in replicate and with local reference ROIs; and (3) scanning angle GCSPRI confers improved dynamic range over fixed angle SPRi approaches, permitting simultaneous detection of small soluble analytes and much larger bacterial cells in the same assay system.

We have demonstrated that the GCSPRI technology can detect protein toxins, bacteria, and viruses in a quantitative manner. Other important considerations for a robust environmental biosensor include reproducibility, specificity, sensitivity and speed of detection. Figures S2 and 4c each demonstrate that equivalent analyte concentrations yield reproducible signals on separate chips and very low deviations were observed among replicates on each sensor chip. Similarly, *B. globigii* samples of equivalent concentration result in comparable signals on different chips, regardless of whether viable or paraformaldehyde-fixed cells were used (Figure S4) or whether samples were diluted in PBS or fish aquarium water (Figures S2 and 4c). While polyclonal antibodies and antisera were shown here to be capable of specific analyte detection, in most cases monoclonal antibodies were used to maximize assay specificity. This label-free real-time biosensor has greater or comparable sensitivity compared to other novel technologies, in that quantitative assessment of M13 virus was possible at 1.1×10^5 PFU/mL; while the Love wave delay line sensor and the quartz crystal microbalance (QCM) (both are instruments based on acoustic waves) have M13 detection limits of 10^9 PFU/mL and 10^6 PFU/mL, respectively [45, 46].

Other ultrasensitive biosensors have been developed for label-free mass-based detection of similar pathogens. In one case, *Vaccinia* virus was aerosolized and neutralized with an electrospray aerosol generator and captured on a QCM crystal, resulting in quantitative viral detection as evidenced by a viral capture rate that displayed linearity with the concentration of initial virus [47]. This study suggested a minimum airborne virus concentration of 40-210 viral particles/mL for QCM detection, but these limits were based upon a relatively high initial viral suspension of 8.5×10^8-8.5×10^{10} PFU/mL in fluid and were calculated using a complex equation that factored in a number of other parameters of the aerosolization procedure. As another example, resonance-based cantilever mechanical pathogen biosensors have been shown to detect the mass equivalent of as few as 1 to 16 *E. coli* cells (0.67 pg - 6 pg total) [48, 49] or even the weight of a single baculovirus particle (~1.5 fg) [50]. It should be noted, however, that these levels of sensitivity for bacterial and viral detection were achieved in air and in a vacuum, respectively, thus minimizing viscous damping that would significantly impact cantilever sensitivity in fluid samples [51]. Moreover, as with the QCM detection of *Vaccinia* virus by Lee et al. [47], the mass equivalent “limit of sensitivity” for baculovirus was extrapolated from data acquired using viral particles suspended in sterile buffer at much higher concentrations (10^5-10^7 PFU/mL) that are closer to those used in our system [50]. Finally, while promising in terms of sensitivity, these micro- or nanoelectromechanical systems (MEMS or NEMS) devices require complex fabrication and functionalization procedures, are of limited utility for detection of analytes in serum or

complex fluids such as environmental samples, and require additional development to enable integration of such sensors with compact detection instrumentation and micro- and nanofluidic systems for future biosensor applications and “lab-on-a-chip” detection systems [51].

The sensitivity of GCSPRI analysis is similar to other published LODs for SPR-based direct detection of bacteria. We have demonstrated GCSPRI detection of live *B. globigii* at 3.2×10^6 cells/mL (Supporting Figure S4) and paraformaldehyde-fixed *B. globigii* at 1.6×10^5 cells/mL (Supporting Figure S5), concentrations that are at or below published LODs (10^6 CFU/ml to 8.7×10^6 CFU/ml) for direct detection of live *E. coli* O157:H7 using three different prism-based SPR instruments [52-54], as well as published LODs (10^6 CFU/ml and 10^7 CFU/ml) for direct detection of live *Listeria* by prism-based SPR sensors [15, 55]. GCSPRI detection of 1.6×10^5 bacterial cells/mL demonstrates a sensitivity within the range of reported levels of *E. coli* in sewage (up to 9.1×10^5 CFU/mL [56]) and within one order of magnitude of reported mean *E. coli* levels in sewage or wastewater (~5×10^4 to more than 10^5 CFU/mL [56-58]). Water samples from highly contaminated rivers have been reported to contain up to 7.9×10^4 fecal coliform bacteria/mL, but this level of environmental contamination is not typical [59]. Further experiments are warranted to evaluate the potential application of GCSPRI analysis for measuring lower levels of environmental contamination, and a number of techniques have been described for improving sensitivity of SPR imaging biosensors [30, 60], including sample preparation methods for bacterial detection [61-63]. For example, sensitivity may be enhanced by enrichment or pre-concentration of pathogenic microbes in environmental samples by techniques such as immunomagnetic separation (IMS) [64] or mechanical size-based concentration using filtration or microfluidics [65]. Most current methods of detection for low abundance pathogens require a pre-concentration step, such as those used for PCR-based detection of enteropathic human adenoviruses [66]. Alternatively, capture of low concentration analytes from larger volumes of sample is also possible as long as background noise is minimized.

In order to demonstrate quantitative detection and estimate limits of detection for bacterial cells by GCSPRI, we used SEM imaging to enumerate the number of captured bacterial cells on the sensor chip and plotted the number of cells counted within each ROI against the GCSPRI angle shift observed at that ROI. Linear correlation analysis of this data resulted in an R^2 value of 0.5988, which, while significant ($p = 0.0052$), is lower than the direct linear correlation we previously reported for GCSPRI capture of mammalian cells [41]. In our previous studies, the larger size of the murine T-cell lymphoma EL4 cells permitted direct visualization and enumeration of captured cells within the sensor chip flowcell imaged using the CCD camera of the GCSPRI instrument.

Our SEM imaging experiments indicate that capture of approximately 90 *B. globigii* results in a GCSPRI angle shift that is two standard deviations above the background GCSPRI value, which, based upon the relative sizes of bacterial and mammalian cells, is consistent with our previous estimate that 1 mammalian cell causes a shift of approximately 1 mDeg [41]. A high level of sensitivity is critical, as ingestion of as few as 60-100 enteropathic O157 *E. coli* bacteria may be sufficient to cause severe infection in humans [67], where fewer than 10^3 CFU/mL of *E. coli* in the blood can be fatal to neonates [68], and where 0.1 to 100 *S. typhi* in blood is associated with acute typhoid fever [69]. Multiplexed GCSPRI assays that include measurements of host analytes that precede the onset of measureable bacterial counts may enable pre-symptomatic diagnosis [70].

The GCSPRI sensor chip active area has the capacity to accommodate over 1000 individual capture spots (ROIs), a dramatic increase in multiplexing capabilities compared to existing

label-free biosensors. This analyte capacity represents a 100-fold increase over the number of sensing channels provided by most prism-based SPR biosensors, and nearly a 10-fold increase over 120-element array-based SPR techniques [71, 72]. In addition to increasing the number of analytes that can be monitored simultaneously and permitting parallel analysis of large numbers of replicate capture spots to improve statistical power, these multiplexing capabilities offer a number of additional advantages. Multiple antibodies against a specific target can be screened in parallel for their relative affinities as well as for potential cross-reactivities. This capability has important ramifications for development of SPR biosensors as well as other immunoassay-based methods of biodetection. The spatially resolved multiplexing of GCSPRI also permits the optimization of additional immunoassay parameters, such as capture reagent type, diluent, and concentration, methods of sensor chip functionalization, and capture molecule immobilization strategies utilizing various surface chemistries, all in parallel on a single sensor chip. Direct visualization of the entire sensor chip by GCSPRI permits the user to define specific regions of interest as well as bare gold negative control ROIs to identify and correct for non-specific binding and effects of bulk shifts in refractive index. These analyses can be performed rapidly using disposable sensor chips that can be mass-produced at low cost and printed in custom microarray format using minimal reagent volumes. Such cost-effective microarray-based biosensors represent a tremendous advantage over expensive high-content oligonucleotide microarrays and high-throughput sequencing instrumentation.

While direct and label-free detection of microbes and their products may be preferable for continuous environmental monitoring, it is also possible to enhance the signal at a given ROI by increasing the local refractive index with secondary antibodies specific for a different epitope on the captured analyte. An additional benefit of this approach could be in the serotyping of bacteria or viral particles. A polyclonal antibody against a pathogen or multiple monoclonal antibodies against different pathogen-associated antigens could be immobilized on a GCSPRI sensor chip that is to be used for continuous on-line monitoring. If an initial binding event results in a positive signal at that capture spot, a serotype-specific secondary monoclonal antibody could then be flowed over the chip, thus increasing sensitivity and further characterizing the captured pathogenic agent. This could prove important in differentiating highly pathogenic serotypes (e.g. O157:H7 *E. coli* or H5N1 avian influenza virus) from less dangerous strains of the same organism. This sandwich-style approach was recently utilized to serotype *Salmonella* by SPR based on somatic O- and flagellar H-antigens [73].

Regarding pathogen detection, one limitation of both immunoassay and nucleic acid-based techniques such as qPCR is difficulty in distinguishing between viable and non-viable microbes. For qPCR based approaches, bacterial samples can be preincubated with propidium monoazide (PMA), which penetrates dead cells, intercalates into the nucleic acid, and after covalent crosslinking via light exposure, prevents DNA from dead cells from being amplified by subsequent PCR [74-78]. This approach, termed PMA-qPCR, has also recently been applied to quantification of viable fungi [79] and RNA enteric viruses [80]. Because GCSPRI represents a label-free technique that does not require cell or viral particle lysis, determination of pathogen viability can easily be achieved after GCSPRI-based detection by eluting captured analytes for downstream analysis, which can include multiplexed PMA-qPCR analysis and/or culture on restrictive media to provide additional insight into genetic information and viability, as has been previously proposed [81]. The benefits of rapid label-free multiplexed screening by GCSPRI microarray can thus be coupled with improved sensitivity and genetic characterization afforded by qPCR analysis and assessment of viability, strain identification, and antibiotic susceptibility or resistance by traditional cultural measurement to enable more thorough characterization of pathogens.

We have shown that multiplexed GCSPRI allows successive or simultaneous detection of a representative virus and a soluble protein in buffer or complex environmental sample matrix. We have also shown the ability of GCSPRI to detect host seroconversion in response to infectious bacteria or pathogen-specific exotoxin by capture of antibodies on the sensor chip. Finally, we have demonstrated a number of benefits of GCSPRI technology as it applies to pathogen detection and have presented a number of experiments to demonstrate important pathogen biosensor attributes such as rapid detection, high-content analysis, quantitative detection, specificity, sensitivity, dynamic range and reproducibility.

Supplementary Material

Refer to Web version on PubMed Central for supplementary material.

Acknowledgments

Work described in this manuscript was supported by grants from the NSF (DM1 0215192), NIH (ES016014) and USDA (58-1940-0-007).

References

1. Ivnitski D, Abdel-Hamid I, Atanasov P, Wilkins E. Biosensors for detection of pathogenic bacteria. Biosensors and Bioelectronics. 1999; 14(7):599.
2. Yang S, Rothman RE. PCR-based diagnostics for infectious diseases: uses, limitations, and future applications in acute-care settings. Lancet Infect Dis. 2004; 4(6):337–48. [PubMed: 15172342]
3. Sergeev N, Distler M, Courtney S, Al-Khaldi SF, Volokhov D, Chizhikov V, Rasooly A. Multipathogen oligonucleotide microarray for environmental and biodefense applications. Biosens Bioelectron. 2004; 20(4):684–98. [PubMed: 15522583]
4. Pozhitkov AE, Tautz D, Noble PA. Oligonucleotide microarrays: widely applied--poorly understood. Brief Funct Genomic Proteomic. 2007; 6(2):141–8. [PubMed: 17644526]
5. Haagmans BL, Andeweg AC, Osterhaus AD. The application of genomics to emerging zoonotic viral diseases. PLoS Pathog. 2009; 5(10):e1000557. [PubMed: 19855817]
6. Ince J, McNally A. Development of rapid, automated diagnostics for infectious disease: advances and challenges. Expert Review of Medical Devices. 2009; 6:641. [PubMed: 19911875]
7. Yongfeng H, Fan Y, Jie D, Jian Y, Ting Z, Lilian S, Jin Q. Direct pathogen detection from swab samples using a new high-throughput sequencing technology. Clin Microbiol Infect. 2011; 17(2): 241–4. [PubMed: 20412188]
8. Brockman JM, Nelson BP, Corn RM. Surface plasmon resonance imaging measurements of ultrathin organic films. Annu Rev Phys Chem. 2000; 51:41–63. [PubMed: 11031275]
9. Soelberg SD, Chinowsky T, Geiss G, Spinelli CB, Stevens R, Near S, Kauffman P, Yee S, Furlong CE. A portable surface plasmon resonance sensor system for real-time monitoring of small to large analytes. J Ind Microbiol Biotechnol. 2005; 32(11-12):669–74. [PubMed: 16283397]
10. Homola, J.; Piliarik, M. Surface Plasmon Resonance Based Sensors. Vol. 4. Springer Berlin Heidelberg; 2006. Surface Plasmon Resonance (SPR) Sensors; p. 45-67.
11. Kretschmann E, Raether H. Radiative decay of non-radiative surface plasmon excited by light. Naturforsh. 1968; 23A:2135–6.
12. Homola J. Surface Plasmon Resonance Sensors for Detection of Chemical and Biological Species. Chemical Reviews. 2008; 108(2):462–493. [PubMed: 18229953]
13. Subramanian A, Irudayaraj J, Ryan T. Mono and dithiol surfaces on surface plasmon resonance biosensors for detection of Staphylococcus aureus. Sensors and Actuators B: Chemical. 2006; 114(1):192.
14. Waswa J, Irudayaraj J, DebRoy C. Direct detection of E. Coli O157:H7 in selected food systems by a surface plasmon resonance biosensor. LWT - Food Science and Technology. 2007; 40(2):187.

15. Koubová V, Brynda E, Karasová L, Škvor J, Homola J, Dostálek J, Tobiška P, Rošický J. Detection of foodborne pathogens using surface plasmon resonance biosensors. Sensors and Actuators B: Chemical. 2001; 74(1-3):100–105.

16. Jyoung JY, Hong S, Lee W, Choi JW. Immunosensor for the detection of Vibrio cholerae O1 using surface plasmon resonance. Biosensors and Bioelectronics. 2006; 21(12):2315–2319. [PubMed: 16326089]

17. Kang CD, Lee SW, Park TH, Sim SJ. Performance enhancement of real-time detection of protozoan parasite, Cryptosporidium oocyst by a modified surface plasmon resonance (SPR) biosensor. Enzyme and Microbial Technology. 2006; 39(3):387–390.

18. Leonard P, Hearty S, Quinn J, O'Kennedy R. A generic approach for the detection of whole Listeria monocytogenes cells in contaminated samples using surface plasmon resonance. Biosens Bioelectron. 2004; 19(10):1331–5. [PubMed: 15046767]

19. Skottrup P, Nicolaisen M, Justesen AF. Rapid determination of Phytophthora infestans sporangia using a surface plasmon resonance immunosensor. J Microbiol Methods. 2007; 68(3):507–15. [PubMed: 17157943]

20. Boltovets PM, Snopok BA, Boyko VR, Shevchenko TP, Dyachenko NS, Shirshov YM. Detection of plant viruses using a surface plasmon resonance via complexing with specific antibodies. J Virol Methods. 2004; 121(1):101–6. [PubMed: 15350739]

21. Gomara MJ, Ercilla G, Alsina MA, Haro I. Assessment of synthetic peptides for hepatitis A diagnosis using biosensor technology. Journal of Immunological Methods. 2000; 246(1-2):13–24. [PubMed: 11121543]

22. Nedelkov D, Nelson RW. Detection of Staphylococcal Enterotoxin B via Biomolecular Interaction Analysis Mass Spectrometry. Appl Environ Microbiol. 2003; 69(9):5212–5215. [PubMed: 12957904]

23. Tsai WC, Li IC. SPR-based immunosensor for determining staphylococcal enterotoxin A. Sensors and Actuators B: Chemical. 2009; 136(1):8–12.

24. Vaisocherová H, Mrkvová K, Piliarik M, Jinoch P, Šteinbachová M, Homola J. Surface plasmon resonance biosensor for direct detection of antibody against Epstein-Barr virus. Biosensors and Bioelectronics. 2007; 22(6):1020–1026. [PubMed: 16797175]

25. Chung JW, Kim SD, Bernhardt R, Pyun JC. Application of SPR biosensor for medical diagnostics of human hepatitis B virus (hHBV). Sensors and Actuators B: Chemical. 2005; 111-112:416–422.

26. Chinowsky TM, Soelberg SD, Baker P, Swanson NR, Kauffman P, Mactutis A, Grow MS, Atmar R, Yee SS, Furlong CE. Portable 24-analyte surface plasmon resonance instruments for rapid, versatile biodetection. Biosensors and Bioelectronics. 2007; 22(9-10):2268. [PubMed: 17223032]

27. Homola J, Lu HB, Nenninger GG, Dostálek J, Yee SS. A novel multichannel surface plasmon resonance biosensor. Sensors and Actuators B: Chemical. 2001; 76(1-3):403–410.

28. Homola J, Yee SS, Gauglitz Gn. Surface plasmon resonance sensors: review. Sensors and Actuators B: Chemical. 1999; 54(1-2):3–15.

29. Dostálek J, Vaisocherová H, Homola J. Multichannel surface plasmon resonance biosensor with wavelength division multiplexing. Sensors and Actuators B: Chemical. 2005; 108(1-2):758–764.

30. Scarano S, Mascini M, Turner AP, Minunni M. Surface plasmon resonance imaging for affinity-based biosensors. Biosens Bioelectron. 2010; 25(5):957–66. [PubMed: 19765967]

31. Lee KH, Su YD, Chen SJ, Tseng FG, Lee GB. Microfluidic systems integrated with two-dimensional surface plasmon resonance phase imaging systems for microarray immunoassay. Biosens Bioelectron. 2007; 23(4):466–72. [PubMed: 17618110]

32. Piliarik M, Vaisocherová H, Homola J. A new surface plasmon resonance sensor for high-throughput screening applications. Biosens Bioelectron. 2005; 20(10):2104–10. [PubMed: 15741081]

33. Beusink JB, Lokate AMC, Besselink GAJ, Pruijn GJM, Schasfoort RBM. Angle-scanning SPR imaging for detection of biomolecular interactions on microarrays. Biosensors and Bioelectronics. 2008; 23(6):839–844. [PubMed: 17962009]

34. Brockman JM, Fernandez SM. Grating-coupled surface plasmon resonance for rapid, label-free, array-based sensing. American Laboratory. 2001; 33(12):37.

35. Unfricht DW, Colpitts SL, Fernandez SM, Lynes MA. Grating-coupled surface plasmon resonance: a cell and protein microarray platform. Proteomics. 2005; 5(17):4432–42. [PubMed: 16222719]
36. Singh BK, Hillier AC. Surface Plasmon Resonance Imaging of Biomolecular Interactions on a Grating-Based Sensor Array. Analytical Chemistry. 2006; 78(6):2009–2018. [PubMed: 16536440]
37. Lu HB, Homola J, Campbell CT, Nenninger GG, Yee SS, Ratner BD. Protein contact printing for a surface plasmon resonance biosensor with on-chip referencing. Sensors and Actuators B: Chemical. 2001; 74(1-3):91–99.
38. Challa S, Barrette R, Rood D, Zinckgraf J, French R, Silbart L. Non-toxic Pseudomonas aeruginosa exotoxin A expressing the FMDV VP1 G-H loop for mucosal vaccination of swine against foot and mouth disease virus. Vaccine. 2007; 25(17):3328–37. [PubMed: 17276557]
39. Geary SJ, Walczak EM. Isolation of a cytopathic factor from Mycoplasma hyopneumoniae. Infect Immun. 1985; 48(2):576–8. [PubMed: 3988348]
40. Schell RF, Lawrence DA. Differential effects of concanavalin A and phytohemagglutinin on murine immunity : Suppression and enhancement of cell-mediated immunity. Cellular Immunology. 1977; 31(1):142–154. [PubMed: 406049]
41. Jin GB, Unfricht DW, Fernandez SM, Lynes MA. Cytometry on a chip: cellular phenotypic and functional analysis using grating-coupled surface plasmon resonance. Biosens Bioelectron. 2006; 22(2):200–6. [PubMed: 16455238]
42. Zhu G, Mayy M, Bahoura M, Ritzo BA, Gavrilenko HV, Gavrilenko VI, Noginov MA. Elongation of surface plasmon polariton propagation length without gain. Opt Express. 2008; 16(20):15576–83. [PubMed: 18825196]
43. Liu, H. Pathogenic Bacterial Sensors Based on Carbohydrates as Sensing Elements. In: Zourob, M.; Elwary, S.; Turner, A., editors. Principles of Bacterial Detection: Biosensors, Recognition Receptors and Microsystems. Springer; New York: 2008. p. 659-687.
44. Taylor AD, Yu Q, Chen S, Homola J, Jiang S. Comparison of E. coli O157:H7 preparation methods used for detection with surface plasmon resonance sensor. Sensors and Actuators B: Chemical. 2005; 107(1):202–208.
45. Tamarin O, Comeau S, Dejous C, Moynet D, Rebiere D, Bezian J, Pistre J. Real time device for biosensing: design of a bacteriophage model using love acoustic waves. Biosens Bioelectron. 2003; 18(5-6):755–63. [PubMed: 12706589]
46. Uttenthaler E, Schräml M, Mandel J, Drost S. Ultrasensitive quartz crystal microbalance sensors for detection of M13-Phages in liquids. Biosensors and Bioelectronics. 2001; 16(9-12):735. [PubMed: 11679251]
47. Lee J, Jang J, Akin D, Savran CA, Bashir R. Real-time detection of airborne viruses on a mass-sensitive device. Appl Phys Lett. 2008; 93(1):13901. [PubMed: 19529841]
48. Ilic B, Czaplewski D, Craighead HG, Neuzil P, Campagnolo C, Batt C. Mechanical resonant immunospecific biological detector. Applied Physics Letters. 2000; 77(3):450–452.
49. Ilic B, Czaplewski D, Zalalutdinov M, Craighead HG, Neuzil P, Campagnolo C, Batt C. Single cell detection with micromechanical oscillators. 2001; 19:2825–2828.
50. Ilic B, Yang Y, Craighead HG. Virus detection using nanoelectromechanical devices. AIP. 2004; 85:2604–2606.
51. Waggoner PS, Craighead HG. Micro- and nanomechanical sensors for environmental, chemical, and biological detection. Lab Chip. 2007; 7(10):1238–55. [PubMed: 17896006]
52. Meeusen CA, Alocilja EC, Osburn WN. Detection of E. coli O157: H7 using a miniaturized surface plasmon resonance biosensor. Transactions of the ASABE. 2005; 48(6):8.
53. Taylor AD, Ladd J, Yu Q, Chen S, Homola J, Jiang S. Quantitative and simultaneous detection of four food borne bacterial pathogens with a multi-channel SPR sensor. Biosensors and Bioelectronics. 2006; 22(5):752–758. [PubMed: 16635568]
54. Subramanian A, Irudayaraj J, Ryan T. A mixed self-assembled monolayer-based surface plasmon immunosensor for detection of E. coli O157:H7. Biosens Bioelectron. 2006; 21(7):998–1006. [PubMed: 15878825]

55. Hearty S, Leonard P, Quinn J, O'Kennedy R. Production, characterisation and potential application of a novel monoclonal antibody for rapid identification of virulent Listeria monocytogenes. Journal of Microbiological Methods. 2006; 66(2):294–312. [PubMed: 16457899]
56. Chung H, Jaykus LA, Lovelace G, Sobsey MD. Bacteriophages and bacteria as indicators of enteric viruses in oysters and their harvest waters. Water Science and Technology. 1998; 38(12): 37–44.
57. Mandilara GD, Smeti EM, Mavridou AT, Lambiri MP, Vatopoulos AC, Rigas FP. Correlation between bacterial indicators and bacteriophages in sewage and sludge. FEMS Microbiol Lett. 2006; 263(1):119–26. [PubMed: 16958859]
58. Moce-Llivina L, Muniesa M, Pimenta-Vale H, Lucena F, Jofre J. Survival of bacterial indicator species and bacteriophages after thermal treatment of sludge and sewage. Appl Environ Microbiol. 2003; 69(3):1452–6. [PubMed: 12620828]
59. Lucena F, Méndez X, Morón A, Calderón E, Campos C, Guerrero A, Cárdenas M, Gantzer C, Shwartzbrood L, Skraber S, Jofre J. Occurrence and densities of bacteriophages proposed as indicators and bacterial indicators in river waters from Europe and South America. Journal of Applied Microbiology. 2003; 94(5):808–815. [PubMed: 12694445]
60. Paul S, Vadgama P, Ray AK. Surface plasmon resonance imaging for biosensing. IET Nanobiotechnol. 2009; 3(3):71–80. [PubMed: 19640160]
61. Taylor, AD.; Ladd, J.; Homola, J.; Jiang, S. Surface Plasmon Resonance (SPR) Sensors for the Detection of Bacterial Pathogens. In: Zourob, M.; Elwary, S.; Turner, A., editors. Principles of Bacterial Detection: Biosensors, Recognition Receptors and Microsystems. Springer; New York: 2008. p. 83-108.
62. Dudak FC, Boyaci IH. Rapid and label-free bacteria detection by surface plasmon resonance (SPR) biosensors. Biotechnol J. 2009; 4(7):1003–11. [PubMed: 19288516]
63. Kretzer, JW.; Biebl, M.; Miller, S. Sample Preparation: An Essential Prerequisite for High-Quality Bacteria Detection. In: Zourob, M.; Elwary, S.; Turner, A., editors. Principles of Bacterial Detection: Biosensors, Recognition Receptors and Microsystems. Springer; New York: 2008. p. 15-30.
64. Chapman PA, Wright DJ, Siddons CA. A comparison of immunomagnetic separation and direct culture for the isolation of verocytotoxin-producing Escherichia coli 0157 from bovine faeces. Journal of Medical Microbiology. 1994; 40(6):424–427. [PubMed: 8006935]
65. Park SM, Huh YS, Craighead HG, Erickson D. A method for nanofluidic device prototyping using elastomeric collapse. Proc Natl Acad Sci U S A. 2009; 106(37):15549–54. [PubMed: 19717418]
66. Jiang SC. Human Adenoviruses in Water: Occurrence and Health Implications. A Critical Review Environmental Science & Technology. 2006; 40(23):7132–7140.
67. Tuttle J, Gomez T, Doyle MP, Wells JG, Zhao T, Tauxe RV, Griffin PM. Lessons from a large outbreak of Escherichia coli O157:H7 infections: insights into the infectious dose and method of widespread contamination of hamburger patties. Epidemiol Infect. 1999; 122(2):185–92. [PubMed: 10355781]
68. Dietzman DE, Fischer GW, Schoenknecht FD. Neonatal Escherichia coli septicemia--bacterial counts in blood. J Pediatr. 1974; 85(1):128–30. [PubMed: 4604810]
69. Wain J, Diep TS, Ho VA, Walsh AM, Nguyen TT, Parry CM, White NJ. Quantitation of bacteria in blood of typhoid fever patients and relationship between counts and clinical features, transmissibility, and antibiotic resistance. J Clin Microbiol. 1998; 36(6):1683–7. [PubMed: 9620400]
70. Lukaszewski RA, Yates AM, Jackson MC, Swingler K, Scherer JM, Simpson AJ, Sadler P, McQuillan P, Titball RW, Brooks TJ, Pearce MJ. Presymptomatic prediction of sepsis in intensive care unit patients. Clin Vaccine Immunol. 2008; 15(7):1089–94. [PubMed: 18480235]
71. Shumaker-Parry JS, Aebersold R, Campbell CT. Parallel, Quantitative Measurement of Protein Binding to a 120-Element Double-Stranded DNA Array in Real Time Using Surface Plasmon Resonance Microscopy. Analytical Chemistry. 2004; 76(7):2071–2082. [PubMed: 15053673]
72. Dostálek J, Homola J. Surface plasmon resonance sensor based on an array of diffraction gratings for highly parallelized observation of biomolecular interactions. Sensors and Actuators B: Chemical. 2008; 129(1):303–310.

73. Mazumdar SD, Barlen B, Kämpfer P, Keusgen M. Surface plasmon resonance (SPR) as a rapid tool for serotyping of Salmonella. Biosensors and Bioelectronics. 2010; 25(5):967–971. [PubMed: 19913402]
74. Wahman DG, Schrantz KA, Pressman JG. Determination of the effects of medium composition on the monochloramine disinfection kinetics of Nitrosomonas europaea by the propidium monoazide quantitative PCR and Live/Dead BacLight methods. Appl Environ Microbiol. 2010; 76(24):8277–80. [PubMed: 20952645]
75. Bae S, Wuertz S. Discrimination of viable and dead fecal Bacteroidales bacteria by quantitative PCR with propidium monoazide. Appl Environ Microbiol. 2009; 75(9):2940–4. [PubMed: 19270114]
76. Nocker A, Sossa KE, Camper AK. Molecular monitoring of disinfection efficacy using propidium monoazide in combination with quantitative PCR. J Microbiol Methods. 2007; 70(2):252–60. [PubMed: 17544161]
77. Nocker A, Mazza A, Masson L, Camper AK, Brousseau R. Selective detection of live bacteria combining propidium monoazide sample treatment with microarray technology. J Microbiol Methods. 2009; 76(3):253–61. [PubMed: 19103234]
78. Nocker A, Camper AK. Novel approaches toward preferential detection of viable cells using nucleic acid amplification techniques. FEMS Microbiol Lett. 2009; 291(2):137–42. [PubMed: 19054073]
79. Vesper S, McKinstry C, Hartmann C, Neace M, Yoder S, Vesper A. Quantifying fungal viability in air and water samples using quantitative PCR after treatment with propidium monoazide (PMA). J Microbiol Methods. 2008; 72(2):180–4. [PubMed: 18160156]
80. Parshionikar S, Laseke I, Fout GS. Use of propidium monoazide in reverse transcriptase PCR to distinguish between infectious and noninfectious enteric viruses in water samples. Appl Environ Microbiol. 2010; 76(13):4318–26. [PubMed: 20472736]
81. Johnson-White B, Lin B, Ligler FS. Combination of Immunosensor Detection with Viability Testing and Confirmation Using the Polymerase Chain Reaction and Culture. Analytical Chemistry. 2006; 79(1):140–146. [PubMed: 17194131]

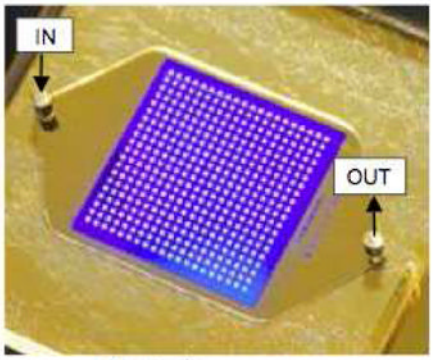

Figure 1a

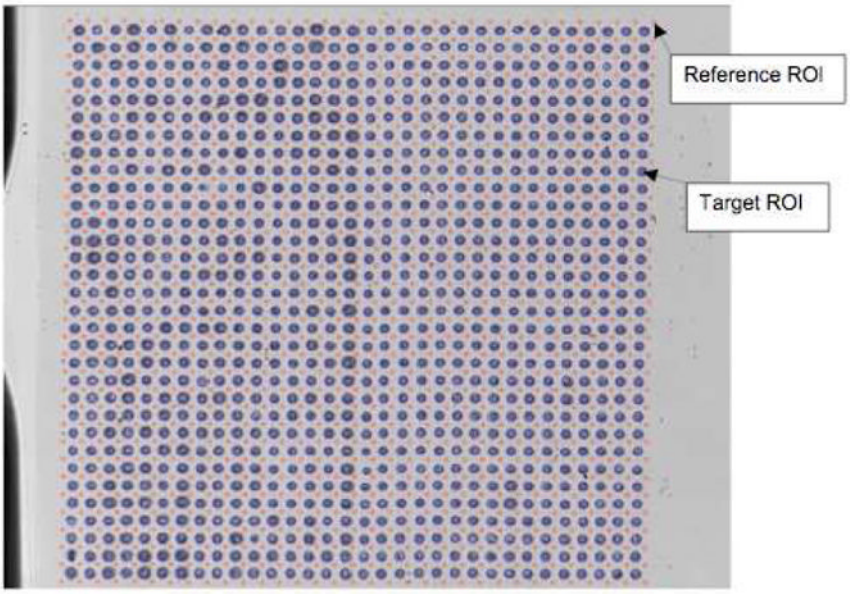

Figure 1b

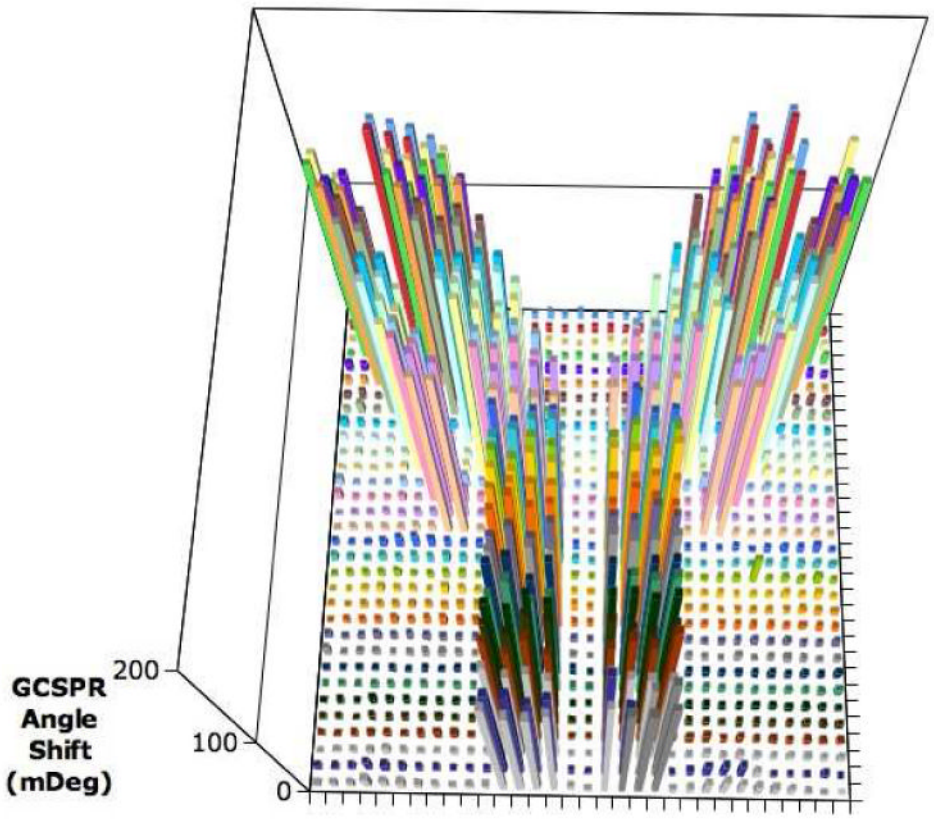

Figure 1c

Figure 1. Scanning Optical Head GCSPRI Sensor Chip Configuration

(a) GCSPRI sensor chip with a 20×20 microarray of antibodies immobilized within the 1 cm^2 active area and a window attached to form flow cell **(b)** BSA and mouse IgG (500 μg/mL**)** were printed in a 32×32 microarray on a sensor chip. Blue ROIs were drawn around each capture spot (~ 110 μm diameter) and red local reference ROIs are interspersed between the capture ROIs on the dry chip image shown. **(c)** A sample of anti-mouse IgG (10 μg/mL) was flowed over the array depicted in (b), resulting in significant angle shifts at mouse IgG ROIs but not at BSA ROIs.

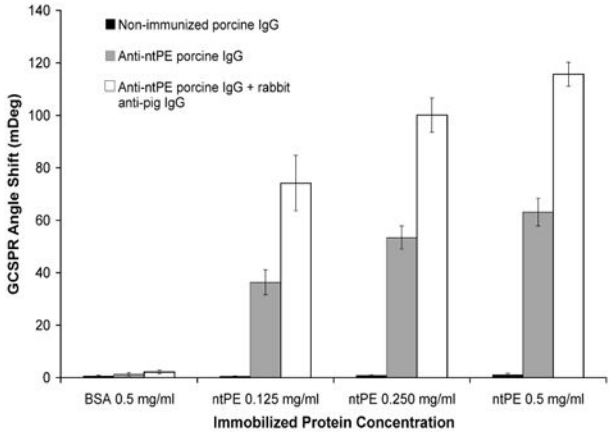

Figure2a

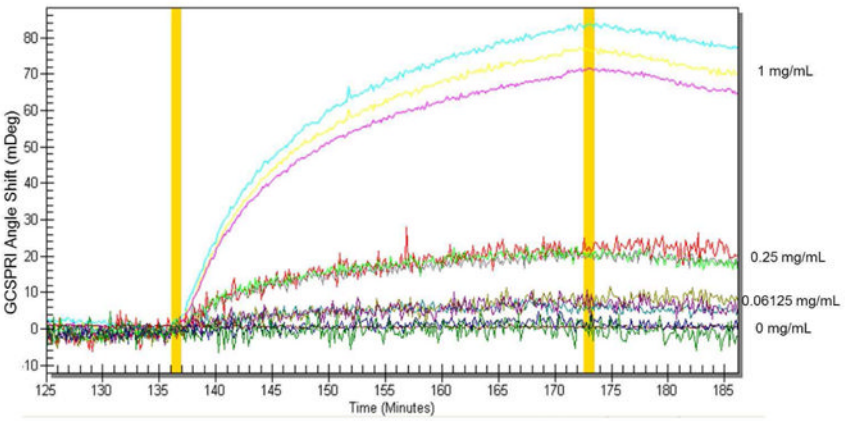

Figure 2b

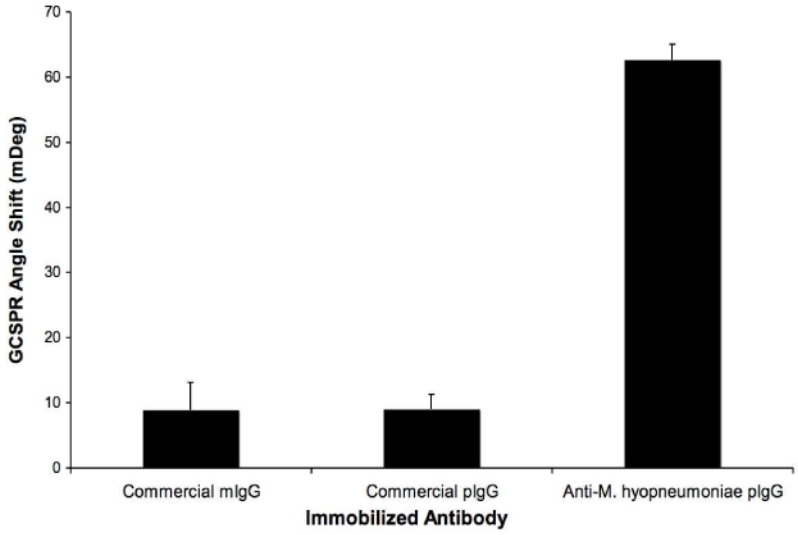

Figure 2c

Figure 2. Specific GCSPRI detection of soluble analytes

(a) Triplicate spots of ntPE were immobilized on a sensor chip and the chip was exposed to a series of IgG antibodies. A 1:100 dilution of IgG from non-immunized pig sera elicited a negligible GCSPRI angle shift (black bars). Subsequent flow of anti-ntPE IgG resulted in GCSPRI angle shifts at ntPE target ROIs only (grey bars). Next, an anti-pig IgG secondary antibody (1:500 dilution) passed over the same surfaces caused a further increase in GCSPRI angle shifts (white bars). **(b)** Total protein from *M. hyopneumoniae* was diluted in 1% Stabilcoat (Surmodics) and immobilized on a sensor chip at the indicated concentrations, each in triplicate. After blocking (10% Superblock), anti-*M. hyopneumoniae* pIgG (162.5 μg/mL) was flowed over the chip, followed by an Fc-specific goat anti-pig IgG antibody (10 μg/mL). The SPR response curve shows the GCSPR angle shift resulting from anti-porcine IgG secondary antibody binding to captured anti-*M. hyopneumoniae* pIgG plotted as a function of time **(c)** Purified IgG antibodies (500 μg/mL**)** from naïve or immunized animals were immobilized in triplicate on the sensor chip. After blocking (10% Superblock), total protein from *M. hyopneumoniae* (100 μg/mL) was delivered to the chip.

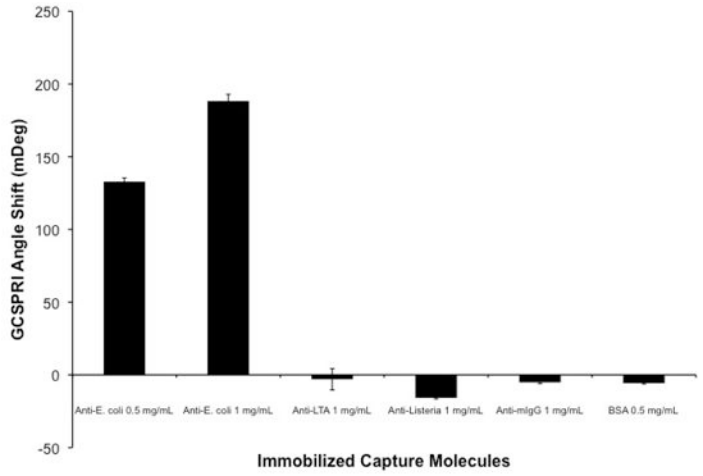

Figure 3a

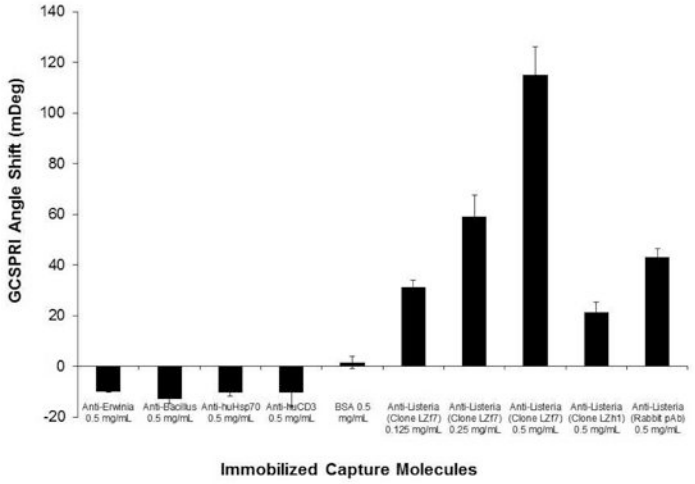

Figure 3b

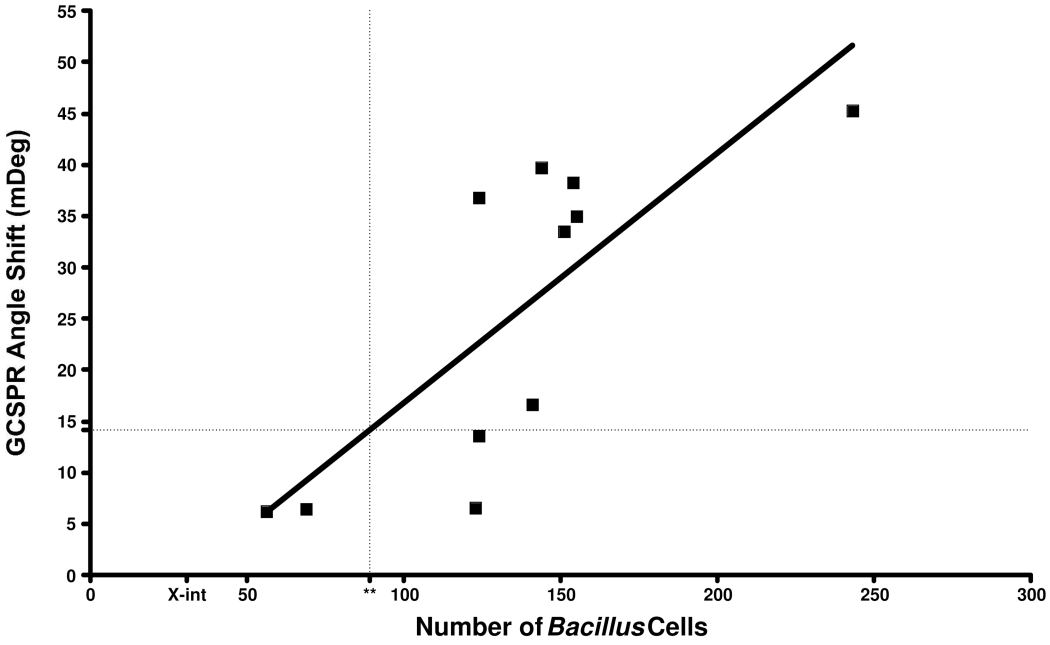

Figure 3c

Figure 3. GCSPRI detection of bacterial cells

(a) Pentuplicate spots of goat polyclonal anti-*E. coli* antibody were immobilized on a sensor chip along with various negative control antibodies. An overnight culture of *E. coli* MC1061 was resuspended in PBST to a concentration of 1×10^8 CFU/mL. After blocking with 5% cold-water teleostean gelatin and establishing a PBST baseline, the *E. coli* sample was flowed over the chip for 30 minutes. **(b)** Triplicate spots of two different monoclonal anti-*Listeria* antibodies, clones LZF7 and LZH1, and a rabbit polyclonal anti-*Listeria* antibody, along with various negative controls, were immobilized at the indicated concentrations on a sensor chip. A sample of heat-killed *Listeria* was resuspended in PBST to a concentration of 1.65×10^9 cells/mL and flowed over the chip. **(c)** *Bacillus globigii* cells were grown overnight in TSB at 37°C, then pelleted, washed, and resuspended in PBST at a concentration of 4×10^7 cells/mL for use as sample. The sensor chip was spotted with anti-*B. globigii* antibodies and negative controls at concentrations ranging from 0-500 μg/mL. The chip was blocked with 2% BSA prior to flowing the bacterial cell sample.Immediately after the GCSPRI capture assay the chip was gently dipped in deionized H_20, air dried, and stored in a desiccated container under vacuum conditions at 4°C until scanning electron microscopy (SEM) imaging. Each ROI on the chip was imaged by SEM (750× magnification). Counts of bacterial cells within ROIs were done using Adobe Photoshop 7.0.1. and plotted against the angle shift at each ROI. Linear correlation analysis was performed with GraphPad Prism 4.0 (GraphPad Software, Inc., La Jolla, CA), resulting in Pearson R = 0.7738, R^2 = 0.5988, P value= 0.0052. Horizontal dotted line represents 2 standard deviations above background (background value = mean of 22 reference ROIs).X-int = X-intercept of linear regression (= 30.92 cells). ** = Number of cells required to yield GCSPRI angle shift two standard deviations above background signal (= 89.29 cells).

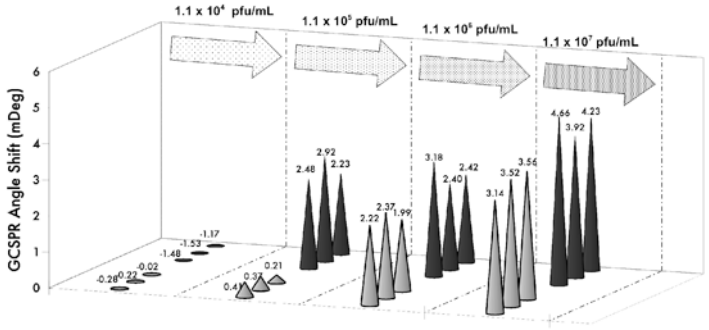

Figure 4a

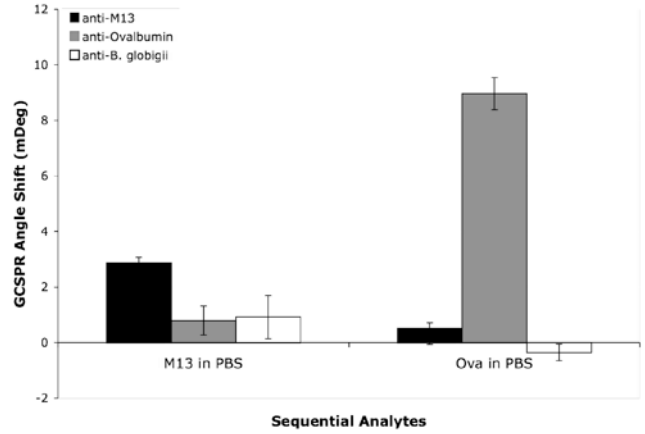

Figure 4b

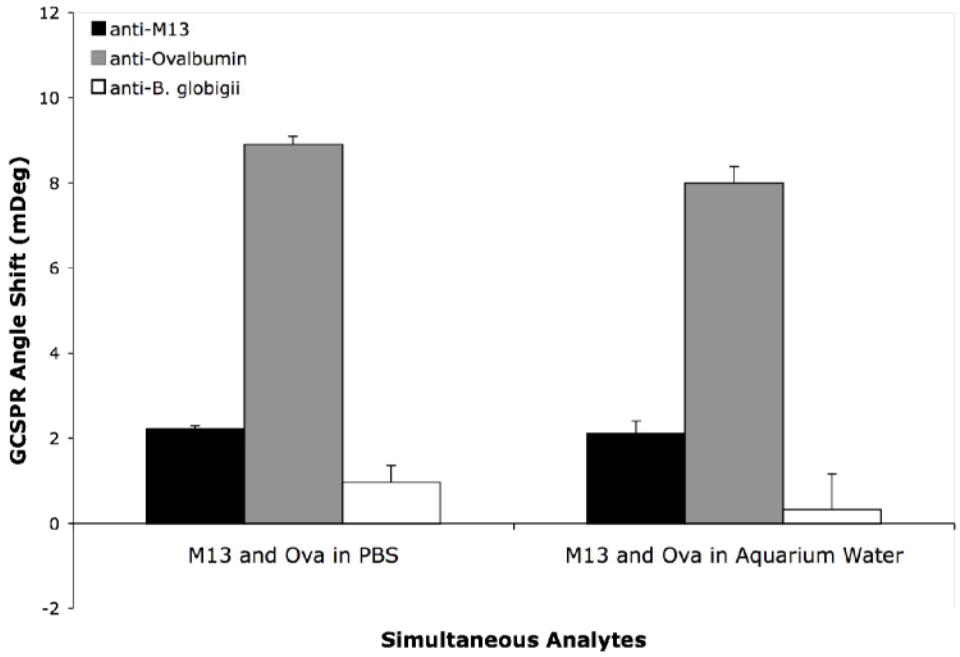

Figure 4c

Figure 4. GCSPRI detection of viral particles at low concentrations and multi-analyte detection in sterile and surrogate environmental samples by GCSPRI

(a) Anti-M13 antibody was immobilized on the sensor chip at concentrations of 0.5 (grey) and 1.0 mg/mL (black), each in triplicate. M13 bacteriophage samples (2 mL) of increasing concentrations (~10^4, 10^5, 10^6, and 10^7 PFU/mL) were recirculated across the chip in succession, each for 20 min with a 10 min PBS wash in between to regenerate a baseline. **(b)** Anti-ovalbumin, anti-M13, and negative control anti-*B. globigii* antibodies (each at 1 mg/mL) were all three immobilized on three separate sensor chips. A 2 mL sample of M13 (10^6 PFU/mL) in PBS was flowed over the first chip for 20 minutes (left group). A 2 mL sample of ovalbumin (Ova) (20 μg/mL) in PBS was then delivered to the same chip (right group). **(c)** A 2 mL sample containing both 20 μg/mL ovalbumin and M13 (10^6 PFU/mL) mixed in PBS was flowed over the second chip (left group). Identical concentrations of ovalbumin and M13 were diluted in 2 mL of freshwater fish aquarium water and delivered to the third chip (right group).